

筑波大学

博士（医学）学位論文

Transcription factor MafB in podocytes
protects against the development of
focal segmental glomerulosclerosis.

(ポドサイトにおける転写因子 MafB は
巣状分節性糸球体硬化症の発症を防ぐ。)

2 0 1 8

筑波大学大学院博士課程人間総合科学研究科

臼井 俊明

CONTENTS

INTRODUCTION

MATERIAL AND METHODS

- *Patients with MAFB mutations*
- *Human kidney tissue samples*
- *Mice*
- *Urinary protein, creatinine and albumin, BUN and serum creatinine*
- *Histopathological analysis of murine renal tissues*
- *Murine Glomerular isolation*
- *Quantitative RT-PCR*
- *RNA-seq*
- *Luciferase assay*
- *Podocyte culture*
- *Statistical Analysis*

RESULTS

- *Duane retraction syndrome (DRS) patients carrying a MAFB mutation develop FSGS associated with the depletion of MAFB in podocytes*
- *MAFB expression in podocytes is decreased in primary FSGS patients*
- *MafB podocyte-specific knockout mice develop overt proteinuria and exhibit focal glomerular segmental sclerosis lesions*
- *Gene expression of slit diaphragm-related proteins (Nphs1 and Magi2) and the podocyte-specific transcription factor Tcf21 is significantly reduced in MafB cKO glomeruli*
- *MafB Directly Regulates Nphs1, Magi2 and Tcf21 Expression*
- *Glomerular expression of MafB targets are decreased in MafB cKO mice and MAFB mutant patients*
- *Enforced overexpression of MafB in podocytes, or treatment with a MafB inducer, protects against FSGS in the murine model*

DISCUSSION

CONCLUSION

ACKNOWLEDGMENTS

REFERENCES

FIGURE

INTRODUCTION

Focal segmental glomerulosclerosis (FSGS) is a common cause of steroid-resistant nephrotic syndrome. Because FSGS is a progressive form of renal disease, it has also become the most common cause of glomerulonephritis-related end-stage renal disease (ESRD). Podocytes are highly specialized visceral epithelial cells that form the outermost layer of the glomerular capillary tufts, and play a critical role in the maintenance of the glomerular filtration barrier. Although FSGS is considered a podocyte disease, the etiology is diverse (1). FSGS due to primary alterations of podocytes can be a result of viral infection, drugs, or genetic disorders. In addition, primary FSGS is diagnosed, by definition, in patients without a known cause (2). Recently, many inheritable genetic forms of FSGS have been described, caused by mutations in proteins that are important for podocyte function. These genes are mainly those regulating slit diaphragm structures, the actin cytoskeleton, foot process structures and transcription factors in podocytes (2).

MafB is a basic leucine zipper transcription factor belonging to the large Maf family (3), which share a conserved basic region and leucine zipper (bZip) motif that mediates dimer formation and DNA binding to the MARE (Maf recognition element) (4). Analysis of MafB-deficient mice revealed that this factor is essential for podocyte differentiation. Nonetheless, MafB expression persists in normal mice after podocyte morphogenesis,

although its role in podocyte maintenance is not well established, because the *MafB*-deficient mice die during the perinatal period (5). Human *MAFB* mutations were reported in multicentric carpotarsal osteolysis (MCTO) and Duane retraction syndrome (DRS) (6, 7). Zankle *et al.* reported that MCTO is caused by mutations clustering within the amino-terminal transcriptional activation domain of *MAFB* (6). MCTO is a rare skeletal dysplasia characterized by aggressive osteolysis, particularly affecting the carpal and tarsal bones, and is frequently associated with progressive renal failure. Because renal biopsy is often only obtained at a late stage of the disease, the relationship between renal involvement and *MAFB* mutation in MCTO has not been clarified (6). Park *et al.* reported that *MAFB* mutations cause DRS (7), which is a congenital eye-movement disorder defined by limited outward gaze and retraction of the eye on attempted inward gaze. It was suggested that in DRS mutants, *MAFB* lacks the domain for DNA binding and dimerization (7). However, Park *et al.* did not report renal involvement in DRS.

Recently, we found that DRS patients carrying a *MAFB* mutation in the DNA-binding domain, p.Leu239Pro, developed FSGS (8). Here, to clarify *MafB* function in podocytes, we investigated conditional podocyte-specific *MafB* knockout (cKO) mice. We found that these mice suffered massive proteinuria and presented with FSGS lesions in the glomeruli. We also found that enforced *MafB* overexpression in podocytes, or

administration of MafB inducers, protected against FSGS.

MATERIAL AND METHODS

Patients with MAFB mutations

This research complied with the Declaration of Helsinki and the Ethics Committee on Human Genome Analysis (ECHGA) of Showa University. Informed written consent was obtained from all patients and their family members.

Human kidney tissue samples

Formalin-fixed paraffin-embedded (FFPE) kidney specimens were obtained from patients with DRS carrying MAFB mutations, minimal change nephrotic syndrome (MCNS), IgA nephropathy (IgAN), primary FSGS and diabetic nephropathy (DN). The clinical study was approved by the Institutional Review Board (IRB) of Fujigaoka Hospital of Showa University School of Medicine (Approved number: F2017C52). This research protocol was also approved by the Ethics Committee of University of Tsukuba Hospital (H26-26). Additionally, the comprehensive permitting system for the treatment of human biological samples at University of Tsukuba Hospital was utilized as a foundation for this research protocol (H26-26). Sections were stained with Periodic acid–Schiff (PAS) and Masson's trichrome (M&T) for histopathological examination under light microscopy. For immunohistochemistry, a standard ABC (avidin-biotin complex) method was employed on

paraffin-embedded sections. Two μm -thick sections were deparaffinized, hydrated, and treated at pH 6.0 in citrate for 10 min (for NPHS1, MAGI2 and TCF21 detection) or pH 9.0 Tris/EDTA (for MAFB and WT1). The tissue was incubated with the following antibodies for 60 minutes at room temperature: mouse anti-MAFB monoclonal antibody (2A6, Life Span Bio Sciences, Seattle, WA, USA; 1:100), rabbit anti-WT-1 monoclonal antibody (CAN-R9(IHC)-56-2, Abcam, Cambridge, UK; 1:200), sheep anti-NPHS1 polyclonal antibody (R&D Systems, Minneapolis, MN, USA; 1:50), rabbit anti-MAGI2 polyclonal antibody (Sigma Aldrich, St. Louis, MO, USA; 1:100) and rabbit anti-TCF21 polyclonal antibody (Abcam; 1:50). The signals were visualized using a horseradish peroxidase-conjugated compact polymer. Diaminobenzidine (DAB) was used as the substrate chromogen. The sections were then counterstained with hematoxylin. For co-immunofluorescence staining of MAFB and WT1, anti-MAFB and anti-WT1 antibodies were labeled with Alexa Fluor-488 (green) and -594 (red) secondary antibodies (Thermo Fisher Scientific, Waltham, MA, USA), respectively. For electron microscopy, tissues were fixed in 2% glutaraldehyde in phosphate-buffered saline, and transmission electron microscopy was performed using standard methods.

Mice

To create MafB conditional knock-out (cKO) mice, the *Mafb* gene was flanked with a loxP element with a neomycin-resistant gene using homologous recombination in ES cells (*Mafb*^{flox/flox}) (9). Following this, the mice were crossed with *NPHS2*-Cre ER^{T2} transgenic mice (10) to obtain *Mafb*^{flox/flox}::*NPHS2*-CRE ER^{T2} animals. Injection of tamoxifen at 6 weeks of age resulted in podocyte-specific MafB knockout. *Mafb*^{flox/flox} mice served as controls. The genetic background of these mice is C57BL/6J. *NPHS1*-MafB transgenic (TG) mice were overexpressing MafB in podocytes by using the *NPHS1* promoter/enhancer (11). These TG mice were backcrossed ten times to BALB/c mice for the adriamycin nephropathy experiments. Mice were maintained in the Laboratory Animal Resource Center. All experiments were performed according to the Guide for the Care and Use of Laboratory Animals of the University of Tsukuba.

Urinary protein, creatinine and albumin, BUN and serum creatinine

Urinary protein, albumin and creatinine were measured in a Hitachi 7170 automated analyzer (Hitachi High-Technologies Corporation, Tokyo, Japan). Urinary protein was determined by the pyrogallol red method, creatinine by an enzymatic method and albumin by turbidimetric immunoassays. BUN and serum creatinine were measured using a

Dry-Chem 3500 automated analyzer for routine laboratory tests (Fuji Film Inc., Tokyo, Japan).

Histopathological analysis of murine renal tissues

Each mouse was bled out while under ether anesthesia. Organs were then fixed with 10% formalin in 0.01 mol/l phosphate buffer (pH 7.2) and embedded in paraffin. Sections were assessed by PAS and M&T staining for histopathological examination under light microscopy. For immunofluorescence analysis, frozen sections were stained using rabbit anti-MafB polyclonal antibody (BL658; BETHYL Laboratories, Montgomery, TX, USA; 1:100), goat anti-Nphs1 polyclonal antibody (R&D Systems; 1:100), rabbit anti-Magi2 polyclonal antibody (Sigma Aldrich; 1:100) and rabbit anti-Tcf21 polyclonal antibody (Abcam; 1:50) using Alexa Fluor-488 (green)-labeled secondary antibodies (Thermo Fisher). Electron microscopy was performed using standard methods. Quantitative estimation of immunofluorescence was performed using Image J software. Relative fluorescence intensity was calculated using the mean fluorescence intensity of wild-type mice defined as 1.0. Glomerulosclerosis score was calculated by dividing the number of sclerotic glomeruli by the total number of glomeruli counted. The degree of glomerular sclerosis was estimated in at least 80 counted glomeruli. The renal tubulointerstitial injury area in each

kidney section was measured using a BIOREVO BZ-9000 microscope (Keyence, Osaka, Japan), and the mean area was calculated. The average foot process width, expressed in microns, was calculated by dividing the total GBM length measured in the single glomerulus by the total number of slits counted. The value obtained was multiplied by $\pi/4$, a correction factor for the random orientation in which the foot processes were sectioned (12).

Murine Glomerular isolation

Mice were anesthetized and perfused through the heart with 1 mg/mL of iron powder (Iron; 1.03815.1000, Merck Millipore, Darmstadt, Germany). Kidneys were minced into small pieces, digested by 10 mg/mL collagenase A (Roche Diagnostics, Basel, Switzerland) and 0.1 mg/mL DNase I (Roche Diagnostics), filtered, and collected using a magnet (13).

Quantitative RT-PCR

Total RNA (1 μ g) was reverse-transcribed into cDNA. Each reaction was done in duplicate. The quantity of cDNA in each sample was normalized to the amount of *Hprt* cDNA. For the PCR, we used SYBR Premix Ex Taq II (TAKARA Bio, Otsu, Japan) according to the manufacturer's instructions. The amplification was carried out in a Thermal Cycler Dice

Real Time System (TAKARA Bio). The following primer pairs were used: *Mafb*, 5'-GTGCAGGTATAAACGCGTCC -3' and 5'-CACCTCCTGCTTAAGCTGCTC -3'; *Hprt*, 5'-CAAACITTTGCTTTCCCTGGT -3' and 5'-CAAGGGCATATCCAACAACA -3'.

RNA-seq

RNA-seq was applied for transcriptome analysis. RNA was extracted from glomeruli from 3 control (*Mafb*^{flox/flox}) and 3 *MafB* cKO mice. Briefly, total RNA was isolated using TRIZOL reagent (ThermoFisher Scientific). RNA quality was controlled using an RNA 6000 Pico kit (Agilent, Santa Clara, CA, USA). A total amount of 50 ng total RNA was used for RNA-seq library preparation using the NEB NEBNext rRNA Depletion Kit and ENBNext Ultra Directional RNA Library Prep Kit (New England Biolabs, Ipswich, MA, USA); 2×36 base paired-end sequencing was performed with NextSeq500 (Illumina, San Diego, CA) by Tsukuba i-Laboratory LLP (Tsukuba, Ibaraki, Japan). FASTQ files were analyzed using CLC Genomics Workbench (Version 7.5.1; Qiagen, Redwood City, CA, USA). Sequences were mapped to mouse genome (mm10) and quantified for annotated genes. Transcription expression values were estimated as “reads per kilobase per million reads,” and analyzed using the Empirical Analysis of the DGE tool (Qiagen). EdgeR, in the statistical software package R (<http://www.rproject.org/>), was used to detect differential gene expression (false

discovery rate <0.05) (14). Functional analysis was performed using Enrichr (<http://amp.pharm.mssm.edu/Enrichr/>)(15). RNA-seq data were visualized on the Integrative Genomics Viewer (IGV) (<http://software.broadinstitute.org/software/igv/>).

Luciferase assay

To construct reporter plasmids, DNA fragments corresponding to positions -2000 to 0 in the WT and mutant murine *Magi2* gene promoter were PCR-amplified and subcloned into the pGL3-Luc vector (Promega, Madison, WI, USA). Additionally, DNA fragments for positions -2080 to +754 in the WT and mutant murine *Tcf21* gene promoter were PCR-amplified. To express MafB, we used a previously-described expression plasmid (pEFX3-FLAG-MafB)(16). Reporter and effector plasmids were transfected into 293T cells by lipofection using polyethylenimine (Polysciences, Warrington, PA, USA) and then harvested 48 hours post-transfection. Luciferase assays were performed according to the manufacturer's protocol using the Dual-Luciferase Reporter Assay System (Promega). Transfection efficiency was routinely monitored and normalized using co-expressed *Renilla reniformis* luciferase activity from the pRL-TK (Promega) expression plasmid.

Podocyte culture

Mouse podocytes (SVI) from a conditionally immortalized cell line were obtained from CLS (CLS GmbH, Eppelheim, Germany) (17). Cells were grown in RPMI 1640 medium supplemented with 10% fetal bovine serum (FBS), penicillin (100 U/L) and streptomycin (100 mg/L) in a controlled humidified atmosphere. To propagate podocytes, the culture medium was supplemented with 10 U/mL mouse recombinant interferon (IFN γ ; R&D Systems) and the cells were cultured at 33°C to enhance the expression of the temperature-sensitive large T antigen (permissive conditions). To induce differentiation, podocytes were maintained at 37°C without IFN γ (non-permissive conditions) for 10 days. Subsequently, podocytes were cultured with *atRA* for 6 hours.

Adriamycin Nephropathy

Male BALB/c mice (WT or TG) aged 8-10 weeks were injected intravenously with a single dose of *adriamycin* (12 mg/kg) (Doxorubicin Hydrochloride; Sigma Aldrich). Urinary protein was measured weekly. The mice were sacrificed 2 weeks after adriamycin administration (18). For MafB induction experiments, *atRA* (all trans-Retinoic Acid; Sigma Aldrich) (320 μ g/mouse) *was injected* intraperitoneally daily for 7 days after adriamycin administration.

Statistical Analysis

All results are expressed as means \pm s.e.m. Significant differences between two groups were analyzed using the unpaired Welch's t-test. Differences were considered statistically significant at $P < 0.05$. Comparisons of survival rates were done by the Kaplan-Meier method and Mantel-Cox log-rank test.

RESULTS

Duane retraction syndrome (DRS) patients carrying a MAFB mutation develop FSGS associated with the depletion of MAFB in podocytes

We recently identified two unrelated Japanese FSGS families including probands suffering from DRS (8). Next-generation sequencing revealed that affected individuals harbored a novel missense variant (p.Leu239Pro) in the *MAFB* DNA-binding domain. The *MAFB* p.Leu239Pro mutation may result in less stable DNA binding. The patients, Case 1 and Case 2, are siblings. The affected sister (Case 1) presented with nephrotic syndrome at the age of 10 years. A renal biopsy at the age of 23 revealed progressive segmental glomerulosclerosis with global tuft obsolescence, severe tubular atrophy and interstitial fibrosis (Fig. 1A). Electron microscopy revealed podocyte foot process effacement (Fig. 1B). The affected brother (Case 2) also developed nephrotic syndrome at the age of 10. A renal biopsy performed at age 18 revealed FSGS. Another patient, Case 3, unrelated to these siblings, was diagnosed by renal biopsy at the age of 17 as suffering from FSGS (Fig. 1A). In these *MAFB* mutation cases, we performed immunohistochemistry for MAFB and WT1 proteins in renal biopsy tissues. Glomerular *podocytes* were identified as *WT1-positive cells*. We confirmed that MAFB is present in podocytes from control glomeruli (from patients with minimal change nephrotic syndrome, MCNS). Meanwhile, MAFB-negative podocytes

(pink-colored) are increased in *MAFB* mutant glomeruli (Fig. 1C). The number of *MAFB*-positive glomerular cells in patients with the mutation was approximately half that of controls. However, the number of podocytes (WT1-positive cells) did not differ between *MAFB* mutants and controls. We found that the number of *MAFB*-positive podocytes in patients carrying the mutation was significantly lower than in controls (Fig. 1D, E).

MAFB expression in podocytes is decreased in primary FSGS patients

Next, we analyzed *MAFB* expression in a variety of human kidney diseases (MCNS, IgA nephropathy, primary FSGS and diabetic nephropathy) (Fig. 2A). We found significantly lower numbers of *MAFB*-positive glomerular cells in primary FSGS and diabetic nephropathy patients relative to those with other kidney diseases (Fig. 2B). After correction for the number of *MAFB*-positive cells-vs-podocyte numbers, the abundance of *MAFB*-positive podocytes in primary FSGS was approximately half that in other kidney diseases (Fig. 2C).

Mafb podocyte-specific knockout mice develop overt proteinuria and exhibit focal glomerular segmental sclerosis lesions

We have determined that human *MAFB* mutation results in FSGS and showed that

MAFB expression in podocytes was decreased in primary FSGS patients. These findings indicate that MAFB plays an important role in podocytes. To investigate the mechanisms related to MafB function in podocytes, we exploited conditional podocyte-specific MafB knockout (cKO) mice (Fig. 3A). We have previously generated *Mafb*^{flox/flox} mice (9) and now we crossed *NPHS2* promoter Cre ER^{T2} transgenic mice (10) with them to create *Mafb*^{flox/flox} :: *NPHS2*-Cre ER^{T2} mice. After injecting tamoxifen at 6 weeks of age, we compared MafB conditional knockout and *Mafb*^{flox/flox} (control) mice. We confirmed that *Mafb* expression in cKO glomeruli was reduced to less than 10% of controls a week after tamoxifen administration (Fig. 3B). After MafB inactivation for 12 weeks following tamoxifen injection, cKO mice showed overt proteinuria (Fig. 3C). The levels of urinary protein in cKO mice were significantly higher than in controls 16 weeks after tamoxifen administration (urinary protein of control versus cKO at 16 weeks: 16.00 ± 1.99 versus 52.04 ± 9.65 (mg/mg creatinine), *P*<0.05) (Fig. 3C). Proteinuria was mainly due to albumin (urinary albumin of control versus cKO at 16 weeks: 0.66 ± 0.36 versus 23.29 ± 5.65 (mg/mg creatinine), *P*<0.05) (Fig. 3D). We examined renal function in MafB cKO mice by measuring blood urea nitrogen (BUN) and serum creatinine as an index of renal function. These mice exhibited significantly higher BUN and serum creatinine levels than control mice 16 weeks after tamoxifen administration (BUN concentration of control versus cKO: 28.8 ± 1.4 versus

36.5 ± 2.2 (mg/dL), $P < 0.01$, serum creatinine concentration of control versus cKO: 0.21 ± 0.02 versus 0.29 ± 0.03 (mg/dL), $P < 0.05$) (Fig. 3E). Fifty percent of the MafB cKO mice were alive at 27.0 ± 3.0 weeks, and most died of renal failure by 40 weeks (Fig. 3F). Their kidneys had a pale appearance (Fig. 3G) and renal histopathological analysis of MafB cKO kidneys showed FSGS lesions 16 weeks after tamoxifen administration (Fig. 3H, J). We also found renal interstitial damage in the MafB cKO mice (Fig. 3H, K). Ultrastructural analysis revealed podocyte foot process effacement in MafB cKO glomeruli (Fig. 3I, L).

Gene expression of slit diaphragm-related proteins (Nphs1 and Magi2) and the podocyte-specific transcription factor Tcf21 is significantly reduced in MafB cKO glomeruli

Because glomerular sclerosis had already occurred in MafB cKO mice 16 weeks after tamoxifen administration, non-specific changes of gene expression in glomeruli would also be expected by that time. Therefore, RNA samples were collected from the isolated glomeruli of MafB cKO and control mice at an earlier time point and RNA-seq analysis was performed (8 weeks after tamoxifen injection). We compared the expression profiles of all 38,924 annotated genes and found that levels of expression of 32 genes were significantly different in MafB cKO mice and controls (False Discovery Rate (FDR) adjusted P -value <

0.05). We observed that 21 genes were down-regulated and 11 up-regulated in MafB cKO glomeruli (Fig. 4A). To investigate potential molecular mechanisms in MafB cKO mice, we performed functional gene enrichment analysis using Enrichr (<http://amp.pharm.mssm.edu/Enrichr/>) (15). This identified down-regulated genes in MafB cKO, ranking 'PodNet: protein-protein interactions in the podocyte' as the top associated process. This involves several podocyte-specific genes including *Nphs1*, *Magi2*, *Tcf21*, *Ddn* and *Angptl2* (Fig. 4B). Interestingly, some of these podocyte-specific genes, *Nphs1*, *Magi2* and *Tcf21*, had already been identified as genetic causes of FSGS or congenital nephrotic syndrome in humans and/or mice (19-23). Therefore, we further analyzed the relationships between *Mafb* and, *Magi2*, *Nphs1*, and *Tcf21*. In our RNA-seq study, the visualization of read mapping clearly showed severe depletion of *Mafb*, *Magi2*, *Nphs1* and *Tcf21* (Fig. 4C). Additionally, we found that podocyte specific genes, *Dag1*, *Iqgap1* and *Ntrk3* were upregulated in MafB cKO glomeruli (Fig. 4A, B).

MafB Directly Regulates Nphs1, Magi2 and Tcf21 Expression

A significant reduction of *Nphs1*, *Magi2* and *Tcf21* mRNA in MafB cKO mice suggests a role for MafB in the regulation of their expression. We previously showed that MafB directly regulates the transcription of *Nphs1* by interacting with the highly conserved

MARE site in its promoter region (11). We found that the 5'-flanking region of *Magi2* contains a half-MARE (Maf recognition element; TGCTGA) that is highly conserved between human and mouse (Fig. 4D). Therefore, we hypothesized that MafB directly binds the *Magi2*-MARE and activates *Magi2* transcription. To test this hypothesis, we transfected a firefly luciferase reporter plasmid construct, containing the murine *Magi2* promoter region together with the MafB expression plasmid, into 293T cells. As expected, the reporter was activated by co-expression of MafB in a dose-dependent manner (Fig. 4E). However, a luciferase reporter plasmid construct in which the *Magi2*-MARE was deleted within the *Magi2* promoter (Mut-Luc) was not activated by MafB (Fig. 4E). We also found that the 5'-flanking region of *Tcf21* contains a half-MARE. By the same analysis with *Tcf21*, we found MafB could activate *Tcf21* transcription (Fig. 4F, G). These results suggest that MafB directly regulates the transcription of *Magi2* and *Tcf21* by interacting with the highly conserved half-MARE.

Glomerular expression of MafB targets are decreased in MafB cKO mice and MAFB mutant patients

We assessed the expression of the MafB target proteins Nphs1, *Magi2* and *Tcf21* by semi-quantitative immunofluorescence analysis in MafB cKO mice. Consistent with the

results of RNA-seq analysis, the amounts of these podocyte proteins were significantly decreased in MafB cKO glomeruli (Fig. 5A). As described above, podocytes of DRS patients with *MAFB* mutations were depleted of MAFB (Fig. 1D, E). Therefore, we also performed immunohistochemistry in the human MAFB mutation cases. MAFB targets (NPHS1, MAGI2 and TCF21) were exclusively expressed in glomeruli in controls but in 3 affected individuals, the expression of these proteins was decreased (Fig. 5B).

Enforced overexpression of MafB in podocytes, or treatment with a MafB inducer, protects against FSGS in the murine model

As described above, MafB deletion results in FSGS in mice and humans. We also documented MAFB depletion in human primary FSGS. These results imply that MafB plays a crucial role in podocyte maintenance and FSGS pathogenesis. Thus, we hypothesized that MafB might be protective against FSGS. To test this, MafB podocyte-specific transgenic (TG) mice were treated with adriamycin which causes nephropathy, an accepted murine model for FSGS (18). We previously generated transgenic (TG) mice as previously described (11). Renal injury was induced in these 8-10 week-old TG and WT (wild-type) mice by intravenous injection of adriamycin (ADR). Renal manifestations were assessed two weeks thereafter. The level of urinary protein in

ADR-induced TG mice (TG ADR) was significantly less than in WT mice (WT ADR) (urinary protein of WT ADR versus TG ADR: 165.22 ± 25.81 versus 34.05 ± 10.68 (mg/mg creatinine), $P < 0.01$) (Fig. 6A). Severe glomerular sclerosis was observed in WT ADR mice, but was less obvious in TG ADR mice (Fig. 6B). We performed RT-PCR analysis on isolated glomeruli and found increased expression of *Mafb* in control (ADR-non-induced) TG (TG Cont) glomeruli relative to WT controls (WT Cont). *Mafb* expression was reduced after induction of ADR nephropathy in WT glomeruli. However, *Mafb* expression in TG ADR glomeruli remained greater than that observed in WT Cont mice (Fig. 6C). Thus, enforced MafB overexpression in podocytes protected against adriamycin-induced podocyte damage and proteinuria.

Recently, we showed that PPAR δ /RXR α , LXR α /RXR α , RAR, and glucocorticoid receptor (GR) agonists activate *Mafb* expression in macrophages. All-trans retinoic acid (atRA), a RAR agonist, particularly strongly induced *Mafb* (24). However, it was not known whether atRA could induce MafB in other cell types or *in vivo*. To determine whether atRA induces MafB expression in murine podocyte cell lines, they were cultured in the presence of atRA 0, 1, 10 or 100 nM. We found that atRA induced *Mafb* expression in cultured podocytes in a dose-dependent manner. The addition of 100 nM atRA increased *Mafb* expression by greater than 10-fold relative to untreated cells (Fig. 6D).

Next, we investigated the effects of atRA on ADR nephropathy. After ADR administration, WT mice were treated with daily intraperitoneal injections of *atRA* for 7 days, or left untreated. The level of urinary protein in atRA-treated ADR-induced (atRA(+)) ADR mice was significantly lower than in atRA-non-treated ADR-induced (atRA(-)) ADR mice (urinary protein of atRA(-)) ADR versus atRA(+)) ADR at 2 weeks: 109.91 ± 19.65 versus 44.55 ± 9.47 (mg/mg creatinine), $P < 0.01$) (Fig. 6E). Glomerular sclerosis was observed in atRA(-)) ADR mice, but was again less obvious in atRA(+)) ADR mice (Fig. 6F). Glomerular *Mafb* expression was significantly reduced in atRA(-)) ADR mice compared with atRA(-)) Cont animals, whereas *Mafb* levels did not significantly differ between atRA(+)) Cont and atRA(+)) ADR mice (Fig. 6G). Thus, atRA inhibits murine FSGS by *Mafb* induction in glomeruli. These data provide new insights into the underlying molecular mechanisms of FSGS and suggest a novel therapeutic strategy.

DISCUSSION

FSGS is a clinicopathologic syndrome manifesting as proteinuria, usually within the nephrotic range, characterized by a typical histological injury pattern, steroid-resistance, and progression to ESRD (1, 2). Treatment of nephrotic syndrome due to FSGS remains a medical challenge because its steroid resistance requires a high cumulative steroid dose.

The necessity of using alternative steroid-sparing immunosuppressive agents with potential toxic side effects also restricts their long-term use. Several other treatments have been explored in steroid-resistant nephrotic patients with FSGS, but to date, these therapies have either not been effective, or there is thus far too little experience of them to determine their ultimate utility (25). In the present study, we identified MafB as a potential novel therapeutic target for FSGS.

MafB is expressed in both developing and mature podocytes. It regulates the later steps of podocyte development at the capillary loop stage or *after* (26). Analysis of MafB-deficient mice shows that it is essential for podocyte differentiation and foot process formation (5). However, its role in podocyte maintenance has not been established, because MafB-deficient mice die during the perinatal period (5). Here, we show conditional MafB podocyte-specific deficient mice results in FSGS. RNA-seq analysis revealed several podocyte-specific genes, *Nphs1*, *Magi2*, *Tcf21*, *Ddn* and *Angptl2* were down-regulated in MafB cKO glomeruli. The *NPHS1* gene, encoding Nephrin, is a major cause of congenital nephrotic syndrome (19); it is specifically located at the slit diaphragm of glomerular podocytes (20). MAGI2 (membrane-associated guanylate kinase, WW, and PDZ domain-containing 2) is also known to be a cause of congenital nephrotic syndrome (21). It is a component of the slit diaphragm of glomerular podocytes, and specifically knocking it

out in mice results in FSGS (22). Although the relationships between the podocyte-specific transcription factor TCF21 and human chronic kidney disease (CKD) are not known, Tcf21 conditional knockout mice do develop FSGS (23). The role of Dendrin (Ddn) in podocytes is controversial. Ablation of Dendrin delays the onset of kidney failure in mice (27), but in contrast, several studies reported that its expression is lower in nephrotic animal models and in human glomerular diseases (28, 29). Dendrin is localized at the slit diaphragm in podocytes, protected from Nedd4-2-mediated ubiquitination by Magi-2 (22). Thus, Dendrin depletion in MafB cKO glomeruli might be caused by Magi2 impairment. Although a previous report indicated that ANGPTL2 was upregulated in podocytes of diabetic human glomeruli (30), Angptl2-deficient mice did not reveal any obvious renal phenotype under normal conditions (31). We also found that podocyte specific genes, Dag1, Iqgap1 and Ntrk3 were upregulated in MafB cKO glomeruli (Fig. 4A, B). Dag1 (Dystroglycan) is expressed by podocytes, but its specific deletion in mice caused only mild GBM thickening, suggesting that it is not a critical adhesion receptor in podocytes (32). Iqgap1 (IQ domain GTPase-activating protein 1) and Nephrin are co-localized in podocytes. Because Iqgap1 regulates actin cytoskeleton organization in podocytes through interaction with Nephrin (33), its increase may be secondary to Nephrin depletion. The role of the fourth moiety, Ntrk3 (neurotrophic receptor tyrosine kinase 3), in podocytes is not

established.

In humans, *MAFB* mutation results in FSGS in DRS and MCTO (6-8). DRS is a congenital eye movement anomaly characterized by impaired horizontal eye movement due to cranial nerve mal-development. However, DRS is heterogeneous, and *MAFB* mutations are present in less than 1% of patients (7). Renal involvement in DRS has not been previously reported except in our own cases (8). In contrast, an important complication of MCTO is nephropathy, which can progress to ESRD. The pathognomonic feature of this syndrome is the excessive reabsorption of carpotarsal bones due to osteoclast activation. Because a recent study reported that *MAFB* mutations were found in all MCTO cases analyzed, it is possible that these mutations in the transcriptional activation domain cause MCTO (6). However, almost all previously reported series with renal biopsies in MCTO patients showed only ESRD on histological examination because of the late presentation to nephrologists, and only one case report presented proven FSGS (34). DRS with FSGS is caused by the DNA-binding domain mutation of *MAFB* (8), whereas MCTO patients generally lack abnormalities in eye movement (6). However, DRS with FSGS patients lack carpotarsal bone involvement. The reason for phenotypic differences between the DNA-binding domain and the transcriptional activation domain of *MAFB* is not clear.

We also found decreased *MAFB* in glomeruli in primary FSGS and diabetic

nephropathy patients. These CKD are the major cause of ESRD leading to dialysis. FSGS is a diverse set of syndromes arising after podocyte injury from different causes, some of which are known but others not (35). Similarly, in diabetic nephropathy, podocytes seem to be quite susceptible to injury leading to their loss (35, 36). Such podocyte depletion seems to be a relatively early event in the evolution of diabetic nephropathy and predicts clinical progression of the disease. It has been established that podocyte loss underlies progression of CKD in both humans and experimental animal models (35, 37). We previously showed that MafB overexpression in podocytes prevents diabetic nephropathy through regulation of slit diaphragm proteins, antioxidant enzymes, and Notch pathways (11). In the present study, we also showed that enforced overexpression of MafB in podocytes, or administration of a MafB inducer, protects against FSGS in the murine model. These results indicate that MafB has a protective role against podocyte injury in CKD.

CONCLUSION

In summary, we have demonstrated that MafB mutation results in FSGS in humans and mice due to the depletion of slit diaphragm-related proteins and podocyte-specific transcription factors. Consistent with this, podocyte-specific MafB overexpression prevents

FSGS. We also found that the RAR agonist atRA enhanced MafB expression in podocytes, and played a protective role in murine FSGS. Therefore, MafB could be a therapeutic target for FSGS.

ACKNOWLEDGMENTS

The author thanks Dr. Kunihiro Yamagata, Dr. Naoki Morito (Department of Nephrology, Faculty of Medicine, University of Tsukuba) and Dr. Satoru Takahashi (Department of Anatomy and Embryology, Faculty of Medicine, University of Tsukuba) as doctoral advisers. The author also thanks Dr. Hisashi Oishi (Department of Comparative and Experimental Medicine (DCEM), Graduate School of Medical Sciences, Nagoya City University), Dr. Takashi Kudo, Dr. Michito Hamada, Dr. Akihiro Kuno, Dr. Keigyou Yoh (Department of Anatomy and Embryology, Faculty of Medicine, University of Tsukuba), Dr. Ryusuke Koshida (Department of Anatomy and Neuroscience, Faculty of Medicine, University of Tsukuba), Dr. Joichi Usui (Department of Nephrology, Faculty of Medicine, University of Tsukuba), Dr. Masafumi Muratani (Department of Genome Biology, Faculty of Medicine, University of Tsukuba), Dr. Yoshinori Sato , Dr. Kiyoko Inui, Dr. Naoto Kawata, Dr. Ashio Yoshimura (Division of Nephrology, Department of Medicine, Showa

University Fujigaoka Hospital), Dr. Yasuhiro Tsukaguchi (Second Department of Internal Medicine, Kansai Medical University), Dr. Hideki Yokoi (Department of Nephrology, Kyoto University Graduate School of Medicine) and Dr. Masato Kasahara (Department of Clinical Research, Nara Medical University Hospital) for valuable suggestions and research-supports. The author also thanks Ms. Masami Ojima, Dr. Hyojung Jeon, Dr. Hossam H. Shawki, Ms. Risa Okada, Ms. Yuki Imamura, Mr. Keigo Asano, Ms. Maho Kanai, Mr. Takaaki Ojima and Mr. Yuki Tsunakawa for their excellent technical assistance.

REFERENCES

1. V. D. D'Agati, F. J. Kaskel, R. J. Falk, Focal segmental glomerulosclerosis. *N. Engl. J. Med.* **365**, 2398-2411 (2011).
2. A.B.Fogo, Causes and pathogenesis of focal segmental glomerulosclerosis. *Nat. Rev. Nephrol.* **11**, 76-87 (2015).
3. K. Kataoka, K. T. Fujiwara, M. Noda, M. Nishizawa, MafB, a new Maf family transcription activator that can associate with Maf and Fos but not with Jun. *Mol. Cell. Biol.* **14**, 7581-7591 (1994).
4. K. Kataoka, M. Noda, M. Nishizawa, Maf nuclear oncoprotein recognizes sequences related to an AP-1 site and forms heterodimers with both Fos and Jun. *Mol. Cell. Biol.* **14**, 700-712 (1994).
5. T. Moriguchi, M. Hamada, N. Morito, T. Terunuma, K. Hasegawa, C. Zhang, T. Yokomizo, R. Esaki, E. Kuroda, K. Yoh, T. Kudo, M. Nagata, D. R. Greaves, J. D. Engel, M. Yamamoto, S. Takahashi, MafB is essential for

- renal development and F4/80 expression in macrophages. *Mol. Cell. Biol.* **26**, 5715-5727 (2006).
6. A. Zankl, E. L. Duncan, P. J. Leo, G. R. Clark, E. A. Glazov, M. C. Addor, T. Herlin, C.A. Kim, B. P. Leheup, J. McGill, S. McTaggart, S. Mittas, A. L. Mitchell, G. R. Mortier, S. P. Robertson, M. Schroeder, P. Terhal, M. A. Brown, Multicentric carpotarsal osteolysis is caused by mutations clustering in the amino-terminal transcriptional activation domain of MAFB. *Am. J. Hum. Genet.* **90**, 494-501 (2012).
 7. J. G. Park, M. A. Tischfield, A. A. Nugent, L. Cheng, S. A. Di Gioia, W. M. Chan, G. Maconachie, T. M. Bosley, C. G. Summers, D. G. Hunter, C. D. Robson, I. Gottlob, E. C. Engle, Loss of MAFB Function in Humans and Mice Causes Duane Syndrome, Aberrant Extraocular Muscle Innervation, and Inner-Ear Defects. *Am. J Hum. Genet.* **98**, 1220-1227 (2016).
 8. Y. Sato, H. Tsukaguchi, H. Morita, K. Higasa, M. T. Tran, M. Hamada, T. Usui, N. Morito, S. Horita, T. Hayashi, J. Takagi, I. Yamaguchi, H. T. Nguyen, M. Harada, K. Inui, Y. Maruta, Y. Inoue, F. Koiwa, H. Sato, F. Matsuda, S. Ayabe, S. Mizuno, F. Sugiyama, S. Takahashi, A. Yoshimura, MAFB Mutation Causes Focal Segmental Glomerulosclerosis with Duane Retraction Syndrome. *Kidney Int.* **94**, 396-407 (2018).
 9. M. T. N. Tran, M. Hamada, M. Nakamura, H. Jeon, R. Kamei, Y. Tsunakawa, K. Kulathunga, Y. Y. Lin, K. Fujisawa, T. Kudo, S. Takahashi, MafB deficiency accelerates the development of obesity in mice. *FEBS Open Bio.* **6**, 540-547 (2016).
 10. H. Yokoi, M. Kasahara, M. Mukoyama, K. Mori, K. Kuwahara, J. Fujikura, Y. Arai, Y. Saito, Y. Ogawa, T. Kuwabara, A. Sugawara, K. Nakao, Podocyte-specific expression of tamoxifen-inducible Cre recombinase in mice. *Nephrol. Dial. Transplant.* **25**, 2120-2124 (2010).

11. N. Morito, K. Yoh, M. Ojima, M. Okamura, M. Nakamura, M. Hamada, H. Shimohata, T. Moriguchi, K. Yamagata, S. Takahashi, Overexpression of MafB in podocytes protects against diabetic nephropathy. *J. Am. Soc. Nephrol.* **25**, 2546-57 (2014).
12. H. J. Gundersen, T. Seefeldt, R. Osterby, Glomerular epithelial foot processes in normal man and rats. Distribution of true width and its intra- and inter-individual variation. *Cell Tissue Res.* **205**, 147-55 (1980).
13. M. Takemoto, N. Asker, H. Gerhardt, A. Lundkvist, B. R. Johansson, Y. Saito, C. Betsholtz, A new method for large-scale isolation of kidney glomeruli from mice. *Am. J. Pathol.* **161**, 799-805 (2002).
14. M. D. Robinson, D. J. McCarthy, G. K. Smyth, edgeR: a Bioconductor package for differential expression analysis of digital gene expression data. *Bioinformatics* **26**, 139–140 (2010).
15. E. Y. Chen, C. M. Tan, Y. Kou, Q. Duan, Z. Wang, G. V. Meirelles, N. R. Clark, A. Ma'ayan, Enrichr: interactive and collaborative HTML5 gene list enrichment analysis tool. *BMC Bioinformatics* **14**, 128 (2013).
16. M. Kajihara, H. Sone, M. Amemiya, Y. Katoh, M. Isogai, H. Shimano, N. Yamada, S. Takahashi, Mouse MafA, homologue of zebrafish somite Maf 1, contributes to the specific transcriptional activity through the insulin

promoter. *Biochem. Biophys. Res. Commun.* **312**, 831-842 (2003).

17. D. Schiwiek, N. Endlich, L. Holzman, H. Holthöfer, W. Kriz, K. Endlich, Stable expression of nephrin and localization to cell-cell contacts in novel murine podocyte cell lines. *Kidney Int.* **66**, 91-101 (2004).
18. V. W. Lee, D. C. Harris, Adriamycin nephropathy: a model of focal segmental glomerulosclerosis. *Nephrology (Carlton)* **16**, 30-38 (2011).
19. M. Kestilä, U. Lenkkeri, M. Männikkö, J. Lamerdin, P. McCready, H. Putaala, V. Ruotsalainen, T. Morita, M. Nissinen, R. Herva, C. E. Kashtan, L. Peltonen, C. Holmberg, A. Olsen, K. Tryggvason, Positionally cloned gene for a novel glomerular protein--nephrin--is mutated in congenital nephrotic syndrome. *Mol. Cell* **1**, 575-582 (1998).
20. V. Ruotsalainen, P. Ljungberg, J. Wartiovaara, U. Lenkkeri, M. Kestilä, H. Jalanko, C. Holmberg, K. Tryggvason, Nephrin is specifically located at the slit diaphragm of glomerular podocytes. *Proc. Natl. Acad. Sci. U.S.A.* **96**, 7962-7967 (1999).
21. A. Bierzynska, K. Soderquest, P. Dean, E. Colby, R. Rollason, C. Jones, C. D. Inward, H. J. McCarthy, M. A. Simpson, G. M. Lord, M. Williams, G. I. Welsh, A. B. Koziell, M. A. Saleem, NephroS; UK study of Nephrotic Syndrome. MAGI2 Mutations Cause Congenital Nephrotic Syndrome. *J. Am. Soc. Nephrol.* **28**, 1614-1621(2017).
22. N. Shirata, K. I. Ihara, K. Yamamoto-Nonaka, T. Seki, S. I. Makino, J. A. Oliva Trejo, T. Miyake, H. Yamada, K. N. Campbell, T. Nakagawa, K. Mori, M. Yanagita, P. Mundel, K. Nishimori, K. Asanuma, Glomerulosclerosis

Induced by Deficiency of Membrane-Associated Guanylate Kinase Inverted 2 in Kidney Podocytes. *J. Am. Soc. Nephrol.* **28**, 2654-2669 (2017).

23. Y. Maezawa, T. Onay, R.P. Scott, L.S. Keir, H. Dimke, C. Li, V. Eremina, Y. Maezawa, M. Jeansson, J. Shan, M. Binnie, M. Lewin, A. Ghosh, J. H. Miner, S. J. Vainio, S. E. Quaggin, Loss of the podocyte-expressed transcription factor Tcf21/Pod1 results in podocyte differentiation defects and FSGS. *J. Am. Soc. Nephrol.* **25**, 2459-2470 (2014).
24. M. T. N. Tran, M. Hamada, H. Jeon, R. Shiraishi, K. Asano, M. Hattori, M. Nakamura, Y. Imamura, Y. Tsunakawa, R. Fujii, T. Usui, K. Kulathunga, C. S. Andrea, R. Koshida, R. Kamei, Y. Matsunaga, M. Kobayashi, H. Oishi, T. Kudo, S. Takahashi, MafB is a critical regulator of complement component C1q. *Nat. Commun.* **8**, 1700 (2017).
25. S. M. Korbet, Treatment of primary FSGS in adults. *J. Am. Soc. Nephrol.* **23**, 1769-1776 (2012).
26. V. Sadl, F. Jin, J. Yu, S. Cui, D. Holmyard, S. Quaggin, G. Barsh, S. Cordes, The mouse Kreisler (Krml1/MafB) segmentation gene is required for differentiation of glomerular visceral epithelial cells. *Dev. Biol.* **249**, 16-29 (2002).
27. A. Weins, J. S. Wong, J. M. Basgen, R. Gupta, I. Daehn, L. Casagrande, D. Lessman, M. Schwartzman, K. Meliambro, J. Patrakka, A. Shaw, K. Tryggvason, J. C. He, S. B. Nicholas, P. Mundel, K. N. Campbell, Dendrin ablation prolongs life span by delaying kidney failure. *Am. J. Pathol.* **185**, 2143-2157 (2015).
28. F. Kodama, K. Asanuma, M. Takagi, T. Hidaka, E. Asanuma, H. Fukuda, T. Seki, Y. Takeda, Y. Hosoe-Nagai, R. Asao, S. Horikoshi, Y. Tomino,

- Translocation of dendrin to the podocyte nucleus in acute glomerular injury in patients with IgA nephropathy. *Nephrol. Dial. Transplant.* **28**, 1762–1772 (2013).
29. K. Asanuma, M. Akiba-Takagi, F. Kodama, R. Asao, Y. Nagai, A. Lydia, H. Fukuda, H. E. Tanaka, T. Shibata, H. Takahara, T. Hidaka, E. Asanuma, E. Kominami, T. Ueno, Y. Tomino, Dendrin location in podocytes is associated with disease progression in animal and human glomerulopathy. *Am. J. Nephrol.* **33**, 537–549 (2011).
 30. H. Sun, J. M. Zheng, S. Chen, C. H. Zeng, Z. H. Liu, L. S. Li, Enhanced expression of ANGPTL2 in the microvascular lesions of diabetic glomerulopathy. *Nephron Exp. Nephrol.* **105**, e117-e123 (2007).
 31. M. Tabata, T. Kadomatsu, S. Fukuhara, K. Miyata, Y. Ito, M. Endo, T. Urano, H. J. Zhu, H. Tsukano, H. Tazume, K. Kaikita, K. Miyashita, T. Iwawaki, M. Shimabukuro, K. Sakaguchi, T. Ito, N. Nakagata, T. Yamada, H. Katagiri, M. Kasuga, Y. Ando, H. Ogawa, N. Mochizuki, H. Itoh, T. Suda, Y. Oike, Angiopoietin-like protein 2 promotes *chronic* adipose tissue inflammation and obesity-related systemic insulin resistance. *Cell Metab.* **10**, 178-188 (2009).
 32. G. Jarad, J. W. Pippin, S. J. Shankland, J. A. Kreidberg, J. H. Miner, Dystroglycan does not contribute significantly to kidney development or function, in health or after injury. *Am. J. Physiol. Renal Physiol.* **300**, F811–F820 (2011).
 33. Y. Liu, W. Liang, Y. Yang, Y. Pan, Q. Yang, X. Chen, P. C. Singhal, G. Ding, IQGAP1 regulates actin cytoskeleton organization in podocytes through interaction with nephrin. *Cell Signal.* **27**, 867-877 (2015).

34. A. Connor, J. Highton, N. A. Hung, J. Dunbar, R. MacGinley, R. Walker, Multicentric carpal-tarsal osteolysis with nephropathy treated successfully with cyclosporine A: a case report and literature review. *Am. J. Kidney Dis.* **50**, 649-654 (2007).
35. R. C. Wiggins, The spectrum of podocytopathies: A unifying view of glomerular diseases. *Kidney Int.* **71**, 1205–1214 (2007).
36. M. E. Pagtalunan, P. L. Miller, S. Jumping-Eagle, R. G. Nelson, B. D. Myers, H. G. Rennke, N. S. Coplon, L. Sun, T. W. Meyer, Podocyte loss and progressive glomerular injury in type II diabetes. *J. Clin. Invest.* **99**, 342–348 (1997).
37. B. Isermann, I. A. Vinnikov, T. Madhusudhan, S. Herzog, M. Kashif, J. Blautzik, M. A. Corat, M. Zeier, E. Blessing, J. Oh, B. Gerlitz, D. T. Berg, B. W. Grinnell, T. Chavakis, C. T. Esmon, H. Weiler, A. Bierhaus, P. P. Nawroth, Activated protein C protects against diabetic nephropathy by inhibiting endothelial and podocyte apoptosis. *Nat. Med.* **13**, 1349–1358 (2007).

FIGURE

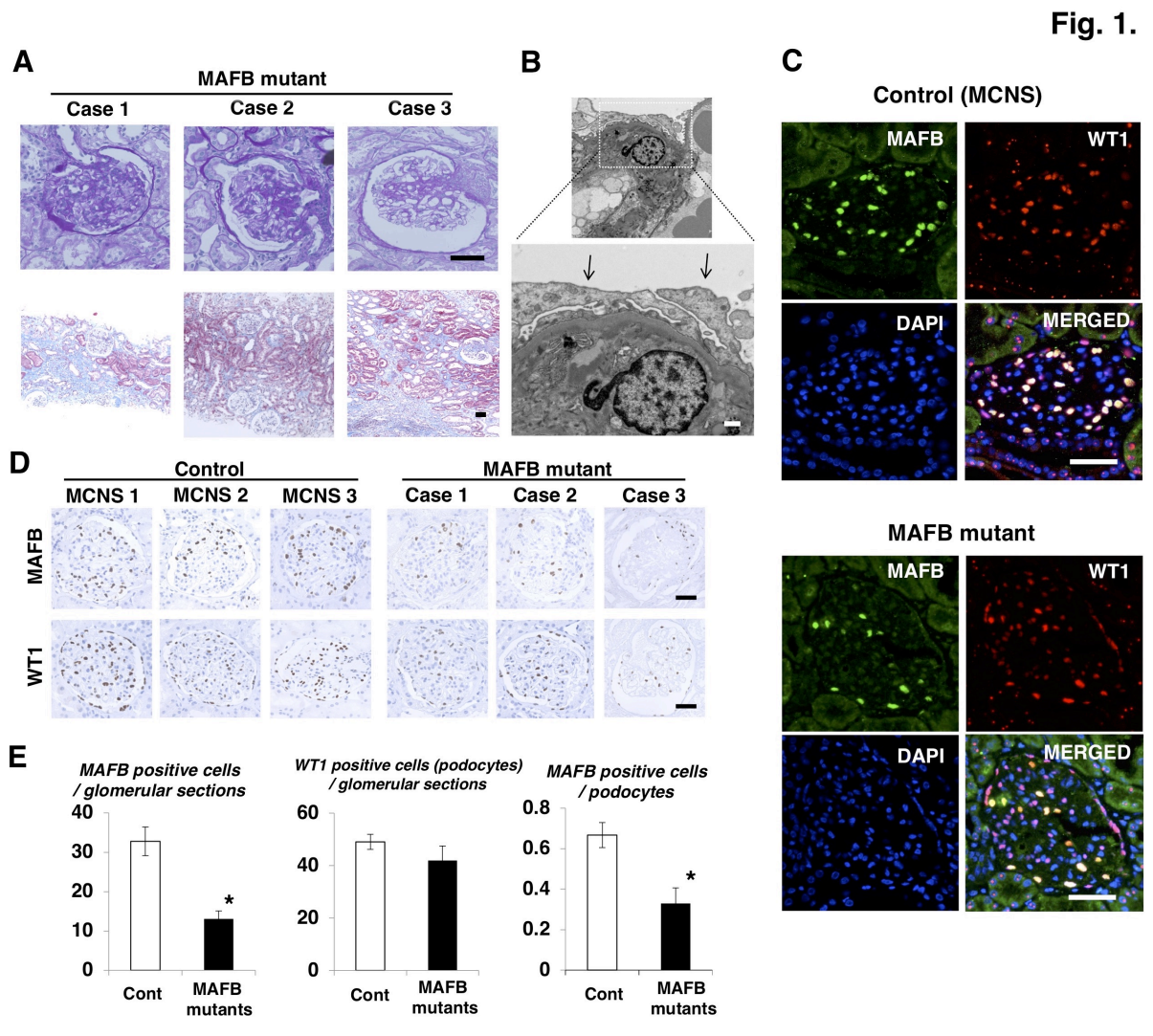


Fig. 1. Patients carrying *MAFB* mutations developed FSGS associated with the decreased *MAFB* expression in podocytes. (A) FSGS lesions in glomeruli of patients carrying the *MAFB* mutation p.Leu 239 Pro. Periodic acid-Schiff (PAS) stain (upper panel). Masson's trichrome staining (lower panel). The blue area, showing fibrosis. Scale bars, 50 μ m. (B) Electron microscopy of podocyte foot process effacement (arrows) in a patient with *MAFB* mutation (Case 1). Scale bar, 2 μ m. (C) *MAFB* expression in podocytes (WT1 positive cells)

of control and MAFB mutant glomeruli. Blue, 4'6-diamidino-2-phenylindole (DAPI); green, MAFB; red, WT1. Scale bar, 50 μ m. Control glomeruli were from a MCNS (minimal change nephrotic syndrome) patient. MAFB mutant glomeruli were from Case 1. (D) Immunohistochemical staining for MAFB and WT1 in renal biopsy specimens from patients with MAFB mutation ($n=3$). Control glomeruli were from MCNS patients ($n=3$). Scale bars, 50 μ m. (E) MAFB-positive cells in podocytes are decreased in MAFB mutant patients: podocytes enumerated as WT1-positive cells. Quantification of MAFB and WT1 staining in all glomerular sections per kidney sample. $n=3$ per group. Values represent the means \pm s.e.m. * $P<0.05$, the unpaired Welch's t-test (E).

Fig. 2.

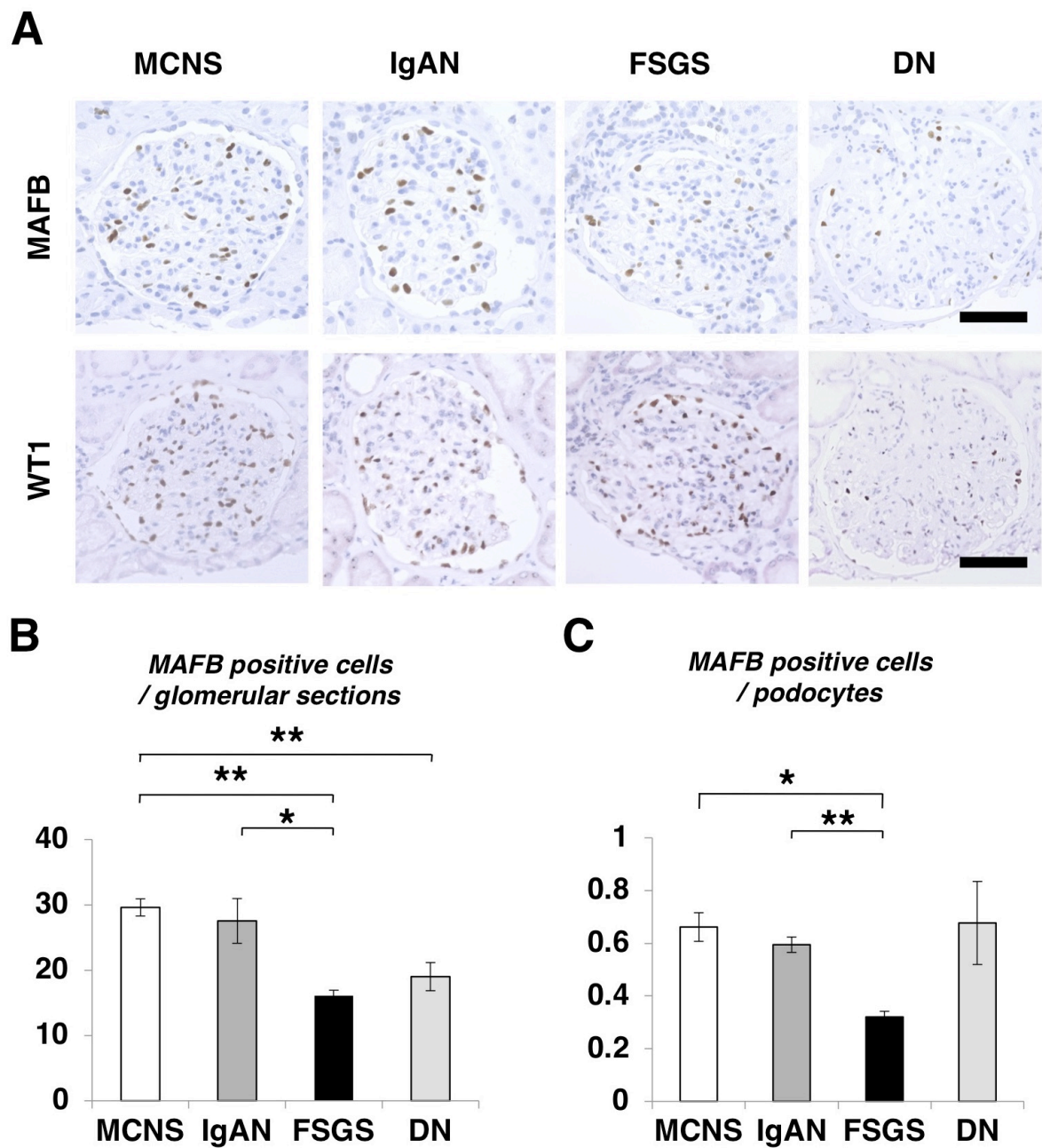


Fig. 2. Glomerular MAFB expression is decreased in primary FSGS patients. (A)

Immunohistochemical staining for MAFB and WT1 in renal biopsy specimens from patients with a variety of kidney diseases. Representative samples are shown. MCNS;

minimal change nephrotic syndrome ($n=3$), IgA nephropathy; IgAN ($n=6$), primary FSGS ($n=6$); FSGS and DN; diabetic nephropathy ($n=5$). Scale bars, 50 μm . (B) Quantification of MAFB staining. (C) Correction of MAFB-positive cell counts by podocyte numbers. Values represent the means \pm s.e.m. * $P<0.05$, ** $P<0.01$, the unpaired Welch's t-test (B, C).

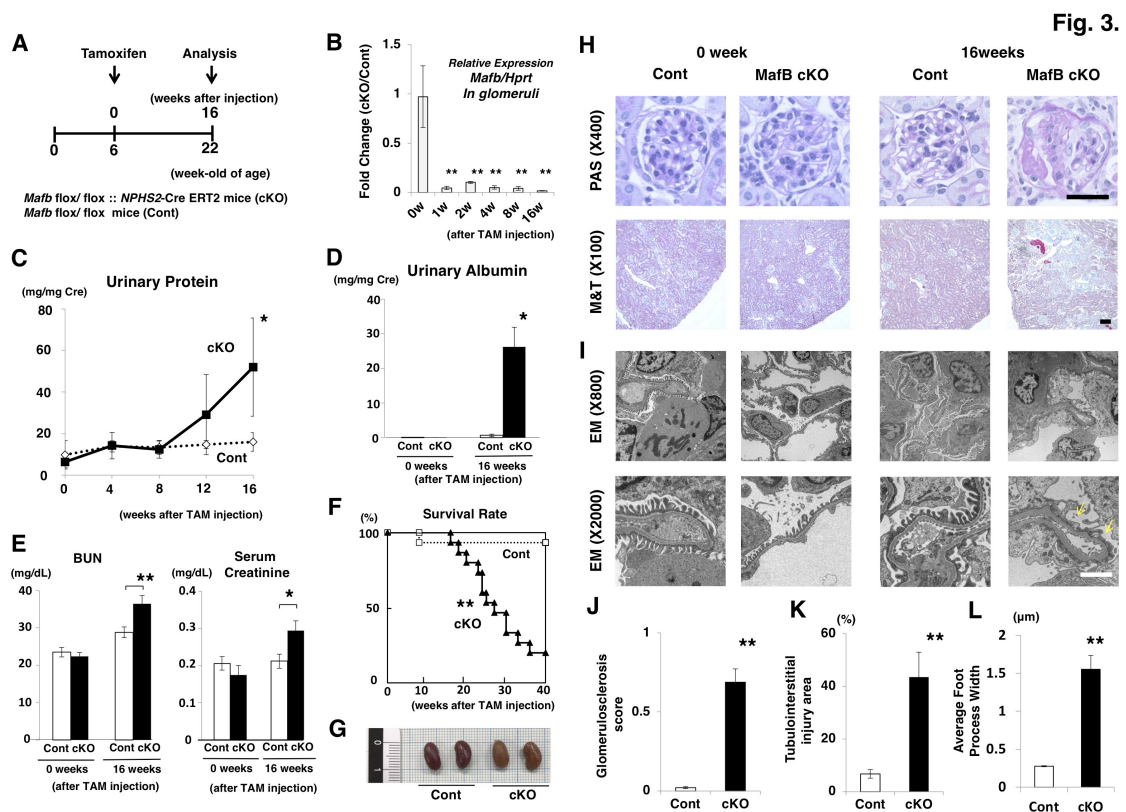


Fig. 3. Podocyte-specific *MafB* knockout mice develop FSGS. (A) Time course of tamoxifen-induced conditional *MafB* deletion. (B) Quantitative RT-PCR analysis. Relative *Mafb* expression in glomeruli after tamoxifen injection. Cont (control; *Mafb*^{flox/flox}) *n*=3; cKO *n*=3. (C) Calculated urinary protein/creatinine ratios in Cont and cKO mice. Cont *n*=5; cKO *n*=6. (D) Calculated urinary albumin/creatinine ratios. Cont *n*=5; cKO *n*=6. (E) BUN and serum creatinine levels. Cont *n*=17; cKO *n*=16. (F) Survival of cKO (*n*=15) and Cont (*n*=15) mice by the Kaplan-Meier method. Fifty percent of cKO mice were alive at 27.0 ± 3.0 weeks. (G) cKO kidneys appearance at 40 weeks. (H) PAS staining (upper panel) and

Masson's trichrome staining (lower panel) in Cont and cKO kidneys. Scale bars, 50 μm . (I)

Ultrastructural analysis. Podocyte foot process effacement (arrows) in cKO glomeruli 16

weeks after tamoxifen administration. Scale bars, 2 μm . (J) Graphs depicting quantitative

analysis of glomerulosclerosis. Glomerulosclerosis score was calculated as (the number of

sclerotic glomeruli)/ (the total number of glomeruli) Cont $n=5$; cKO $n=5$. (K)

tubulointerstitial injury area in Cont and cKO kidneys. Cont $n=5$; cKO $n=5$. (L) The average

foot process width. Cont $n=8$; cKO $n=8$. Each bar represents the mean \pm s.e.m. * $P<0.05$, **

$P<0.01$, the unpaired Welch's t-test (B-E, J-L), Mantel-Cox log-rank test (F).

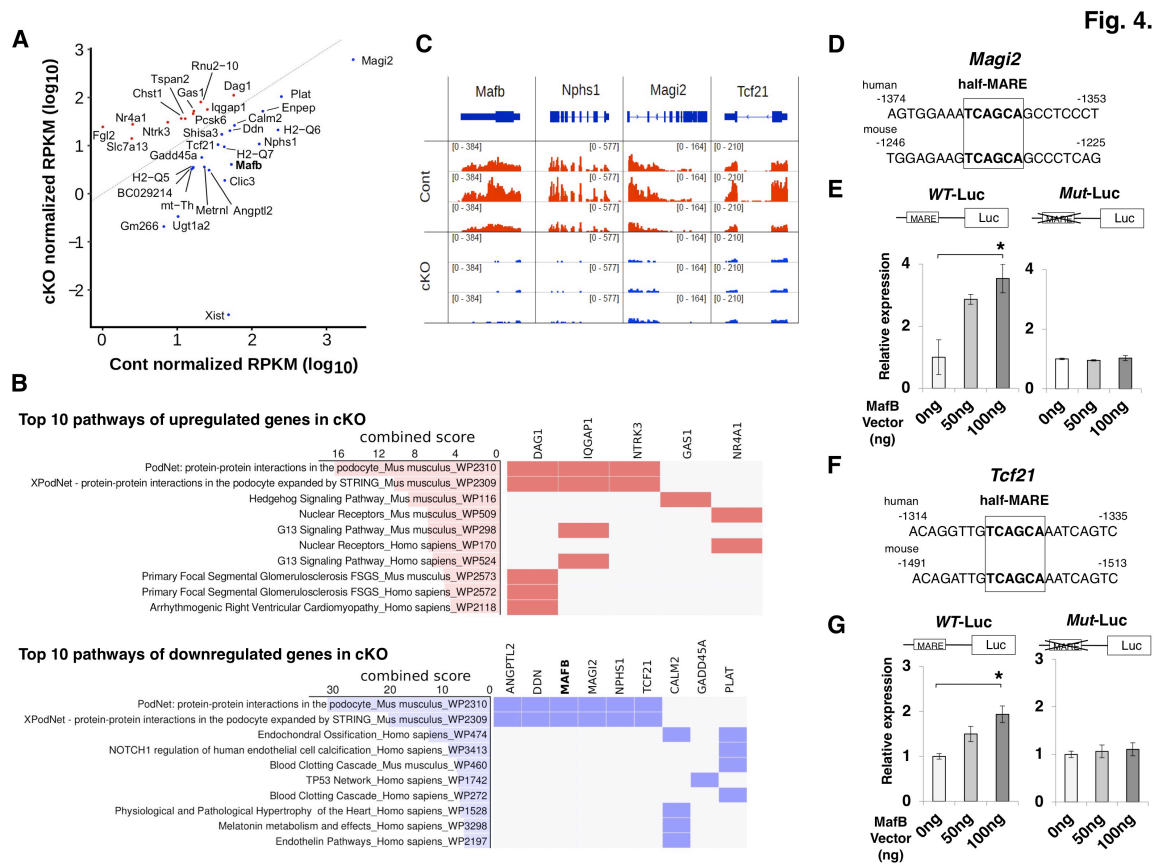


Fig. 4. MafB directly regulates slit diaphragm-related proteins and a podocyte-specific transcription factor. (A) Scatter plot analysis of 32 differentially expressed genes in control (*MafB*^{flox/flox}) and MafB cKO glomeruli. RNA expression levels were calculated as RPKM (reads which map per kilo-base of exon model per million mapped reads). The horizontal axis indicates the RPKM value in Cont (control) glomeruli and the vertical axis the cKO glomeruli. The expression levels of 32 genes were significantly different in cKO mice and controls (FDR adjusted P value < 0.05). Up-regulated genes are plotted as red dots, down-regulated as blue. *n*=3 mice per group. (B) Functional analysis using Enrichr

(<http://amp.pharm.mssm.edu/Enrichr/>). The Wiki Pathway of these 32 genes revealed that podocyte-related genes were mainly affected. (C) RNA-seq read mapping on the loci of 4 podocyte-specific genes (*Mafb*, *Nphs1*, *Magi2* and *Tcf21*). RNA-seq data were visualized on the Integrative Genomics Viewer (IGV) (Cont $n=3$; cKO $n=3$). (D) MafB directly regulates *Magi2* expression. Analysis of the 5'-flanking region of *Magi2* using the Ensembl Genome Database website identified a MafB binding site (half-MARE) that is highly conserved between mouse and human. (E) Reporter assay. Wild-type *Magi2*-MARE (WT-Luc) and mutated *Magi2*-MARE (Mut-Luc) luciferase reporter constructs are indicated. The 293T cells were co-transfected with the indicated *Magi2* promoter-reporter plasmid constructs together with the MafB expression plasmid, and relative luciferase activity was measured as described in *MATERIAL AND METHODS*. (F) MafB directly regulates *Tcf21* expression. Analysis of the 5'-flanking region of *Tcf21*. (G) Reporter assay of *Tcf21*. Each bar represents the mean \pm s.e.m. of duplicates. * $P<0.05$. The data are from one experiment that is representative of at least three independent experiments. Each bar represents the mean \pm s.e.m. * $P<0.05$, the unpaired Welch's t-test (E, G).

Fig. 5.

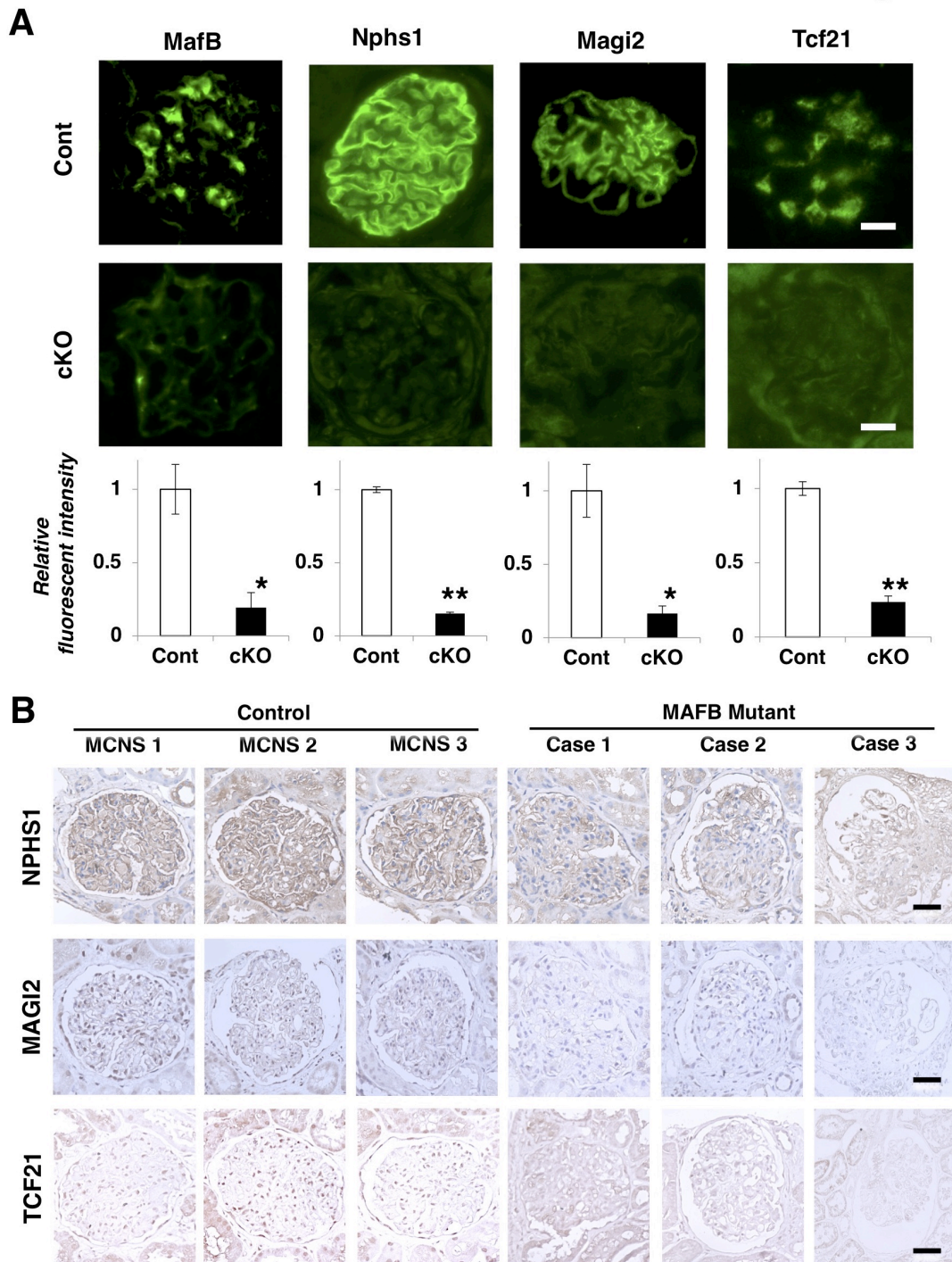


Fig. 5. MafB target proteins are decreased in MafB cKO mice and MAFB mutant patients.

(A) Immunofluorescence analysis. The expression of MafB, Nephryn, Magi2 and Tcf21 in

MafB cKO mice 16 weeks after tamoxifen injection. Graphs depict semi-quantitative analysis by immunofluorescence. Cont $n=3$; cKO $n=3$. (B) MAFB target expression in patients with a *MAFB* mutation. Immunohistochemical staining for NPHS1, MAGI2 and TCF21 in renal biopsy specimens from patients with *MAFB* mutation ($n=3$). NPHS1 and MAGI2 are stained in glomerular tufts, TCF21 in nuclei. Controls were MCNS patients ($n=3$). Scale bars, 50 μm . Each bar represents the mean \pm s.e.m. * $P<0.05$, ** $P<0.01$, the unpaired Welch's t-test (A).

Fig. 6.

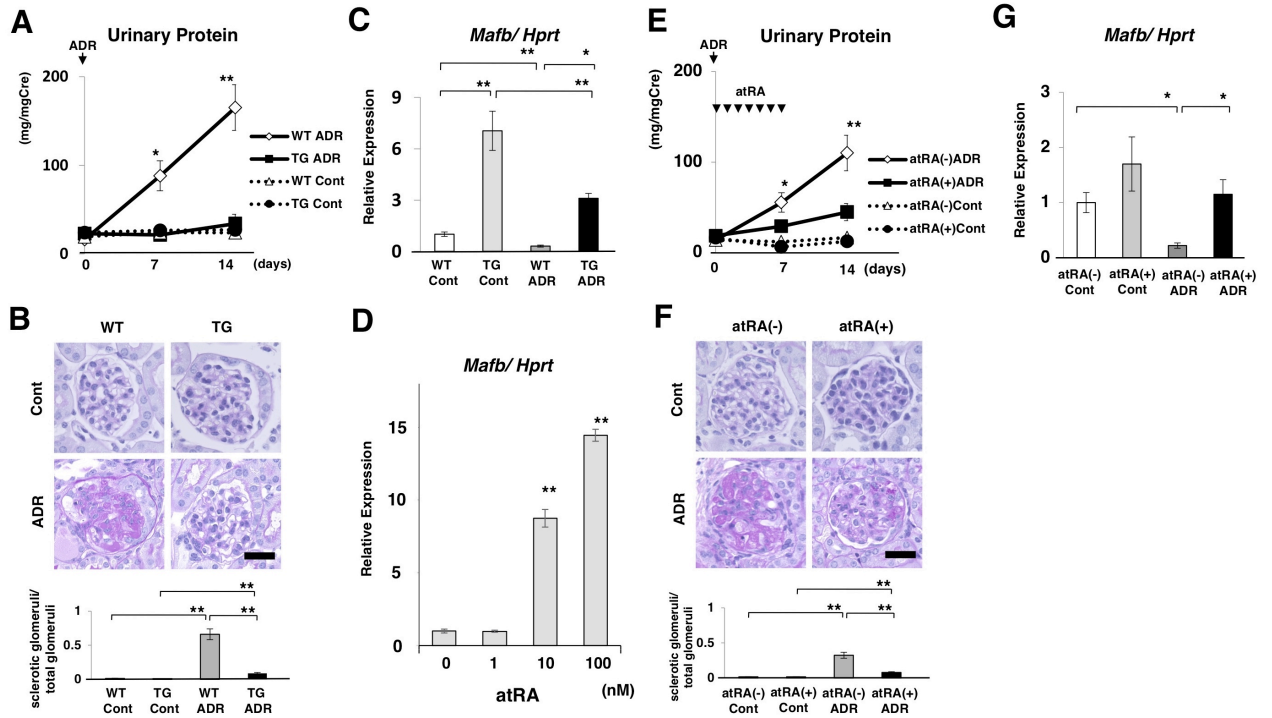


Fig. 6. MafB enforced overexpression, or treatment with a MafB inducer, protects against

FSGS in mice. (A) Calculated urinary protein/creatinine ratios. Adriamycin (ADR)

nephropathy was induced in MafB podocyte-specific transgenic (TG) and WT mice. WT

Cont (ADR(-)), $n=4$; TG Cont (ADR(-)), $n=6$; WT ADR (ADR(+)), $n=6$; TG ADR (ADR(+)), $n=7$.

(B) Histological analysis. Glomerulosclerotic lesions caused by adriamycin nephropathy.

Scale bar, 50 μm . Graphs depict a quantitative analysis of glomerulosclerosis. WT Cont,

$n=4$; TG Cont, $n=4$; WT ADR, $n=4$; TG ADR, $n=4$. (C) Glomerular *Mafb* expression in

adriamycin nephropathy. WT Cont, $n=4$; TG Cont, $n=5$; WT ADR, $n=5$; TG ADR, $n=5$. (D)

atRA induced *Mafb* expression in cultured podocytes. Cells were treated with different

concentrations of atRA for 6 h and RT-PCR analysis of *Mafb* mRNA conducted. The data are from one experiment that is representative of at least two independent experiments. (E) Calculated urinary protein/creatinine ratios. atRA effects in adriamycin nephropathy induced in WT mice (atRA-treated or corn oil-treated). atRA(-) Cont, $n=5$; atRA(+) Cont, $n=6$; atRA(-) ADR, $n=13$; atRA(+) ADR, $n=17$. (F) Quantitative analysis of glomerulosclerosis. Scale bar, 50 μm . atRA(-) Cont, $n=4$; atRA(+) Cont, $n=5$; atRA(-) ADR, $n=5$; atRA(+) ADR, $n=5$. (G) Glomerular *Mafb* expression. atRA administration effect in adriamycin nephropathy. atRA(-) Cont, $n=4$; atRA(+) Cont, $n=5$; atRA(-) ADR, $n=5$; atRA(+) ADR, $n=5$. Each bar represents the mean \pm s.e.m. * $P<0.05$, ** $P<0.01$, the unpaired Welch's t-test (A-G).